



## Journal of Advanced Research in Applied Mechanics

Journal homepage:  
[https://semarakilmu.com.my/journals/index.php/appl\\_mech/index](https://semarakilmu.com.my/journals/index.php/appl_mech/index)  
ISSN: 2289-7895



# MRR and TWR Study of Powder Mix EDM and Pure EDM Based on Response Surface Methodology

Zakaria Mohd Zain<sup>1</sup>, Mir Akmam Noor Rashid<sup>1</sup>, Sher Afghan Khan<sup>2,\*</sup>, Ahsan Ali Khan<sup>1</sup>

<sup>1</sup> Department of Manufacturing & Materials Engineering, International Islamic University Malaysia, Selangor, Gombak-53100, Malaysia

<sup>2</sup> Department of Mechanical Engineering, International Islamic University Malaysia, Selangor, Gombak-53100, Malaysia

### ARTICLE INFO

#### Article history:

Received 17 December 2022

Received in revised form 1 February 2023

Accepted 8 February 2023

Available online 23 February 2023

#### Keywords:

Powder-mixed electrical discharge machining; tantalum carbide powder; SUS 304 stainless steel; MRR

### ABSTRACT

Powder-mixed electrical discharge machining (PMEDM) is the process of enhancing the output of the machined surface by combining dielectric fluid with various types of powders. This process is quickly gaining acceptance in the electrical discharge machining (EDM) sector. The purpose of this study is to determine whether a dielectric fluid containing tantalum carbide (TaC) powder can improve material removal rate (MRR) also lessen tool wear rate (TWR) during the subsequent EDM machining of stainless steel material. During the machining, the material removal rates, tool wear rate, and mathematical models of two different EDM mediums were examined. For the machining procedure, kerosene dielectric fluid containing TaC powder at a concentration of 25.0 g/L was used. The machining input variables were used peak current, pulse on time, and pulse off time. We determined how these variables affected the MRR and TWR of the copper-based EDMed electrode tools. During electrical discharge machining, the MRR for stainless steel (SUS 304) was increased by MRR<sub>PMEDM</sub> by 4.3 to 5.3% and TWR<sub>PMEDM</sub> was reduced by 37.9% when TaC powder additive was used. Optimized results also show that TWR and maximum MRR can be achieved at 81.98% and 13.779mm<sup>3</sup>/min respectively with 83.50% desirability whenever the pulse on-time and pulse off-time are 6.20  $\mu$ s and 6.50  $\mu$ s respectively. The models are reliable and can be used to forecast the machining responses within the experimental region, it can be said. The MRR and TWR model for EDM with TaC powder additive (MRR<sub>PMEDM</sub>) identifies current as the most significant factor, followed by pulse on time and pulse off-time.

## 1. Introduction

The tool and die industry make use of electrical discharge machining (EDM), which is one of the most popular alternative machining methods. When cutting out complicated shapes or materials with high strengths or hardnesses, this method is the one that is utilized most frequently [1-3]. It is almost becoming common practice to use this method for the production of prototypes as well as some manufactured products and parts, most commonly in applications involving low-volume production. Electrical sparks or discharges are produced during the process, and there is only a very

\* Corresponding author.

E-mail address: [sakhan@iium.edu.my](mailto:sakhan@iium.edu.my)

<https://doi.org/10.37934/aram.103.1.1326>

narrow gap between the workpiece and the tool electrode. Extremely delicate materials and sections can be machined without the risk of deformation because they are not in direct physical contact with one another. The addition of powder to the EDM process's dielectric fluid is a recent improvement [4,5]. PMEDM and AEDM are other names for this process [6].

PMEDM uses electrically conductive powder and dielectric fluid to increase sparks between the tool and the workpiece and lower the fluid's insulating strength [7-9]. This method improves dielectric fluid breakdown. During PMEDM, the particles in the dielectric make it much easier for the fluid to break down, which makes it more likely that secondary discharges will happen. This causes the discharge channel to branch off in more than one way. At the points where the electrical pulses hit the electrodes, there will be high temperature and pressure in the gap between them. The high temperature causes the material on the electrodes to melt, which then blows into the dielectric fluid as the discharge quickly stops, one step at a time [10]. As a result, the hot particles closest to the discharge channel move faster through the pool of molten metal. The polarization of particles to form chain-like structures makes it easier for electrons to move, which makes secondary discharges more likely. When molten material is forced into the dielectric, it immediately solidifies into debris, which is carried away by the dielectric fluid's flushing action [11]. Depending on how well the material is flushed, it may re-solidify on the machined surface to form an appendage alloyed film called the recast layer (RL, white/reform layer).

Machining stability improves EDM outputs like MRR, TWR, and SR [5]. The wider discharge gap, which helps to keep the flushing of debris on a more even keel, is what makes stability possible. Research has been carried out to look into how different powders influence the performance of EDM. A few examples of these include aluminum, titanium carbide, silicon, aluminum oxide, titanium dioxide, molybdenum disulfide, nickel, and many other powders that are also used in micro or nanoforms. The increased peak current and  $Al_2O_3$  powder reduced tool wear, according to Khan *et al.*, [12]. TiC had lower layer thickness, greater hardness, and carbon depositions than  $Al_2O_3$  powder. PMEDM uses Al powder extensively. Singh *et al.*, [14] studied the effects of electric parameters on hastelloy machining performance. It has also been used with kerosene to machine cobalt-tungsten carbide. Surfactant and conductive Al powders were used in kerosene dielectric during SKD steel machining [13,14]. Adding powder to dielectric fluids increased MRR, decreased TWR, and increased SR. Powder concentrations and sizes affected machining outputs. Graphite powder was used in the dielectric to improve Inconel 718 and WC-Co machining [15,16]. The cold-treated copper electrode powder reduced TWR and improved Ra and MRR at the nano level. Chatha *et al.*, [17] raised the workpiece's MRR with  $TiO_2$  powder in dielectric fluid. They also noticed that powder-derived elements migrated to the machined surface. Mixing silicon powder with dielectric fluid produces mirror-like EDM surfaces [18]. Kansal *et al.*, [19] found it had the best machining performance. The above studies on EDM output parameters show how Powder mix EDM (PMEDM) was used to improve MRR, surface finish, and TWR. Furutania *et al.*, [20] studied how dielectric fluid powders behaved when machined. They also coated the workpiece with dielectric oil-dissolved powders. During EDM of stainless steel, they used  $MoS_2$  in the dielectric fluid to lubricate space-exposed sliding parts. From these writings, it's clear that various powders have been used to improve machining and EDMed surfaces. Tantalum carbide (TaC) powder in the dielectric fluid may reduce stainless steel tool wear, but more research is needed. This study uses SUS 304 stainless steel. This adaptable and widely used steel grade is used in kitchen benches and utensils, food processing equipment, and chemical environments requiring low machining wear. Formability and weldability make it versatile.

The authors investigated the viability of TaC powder EDM electrodes and the effect of powder concentration on MRR and TWR outputs. The current research investigates the MRR and its

mathematical modeling using PMEDM with TaC powder in the dielectric fluid to find the most efficient input parameter.

## 2. Materials and Methodology

### 2.1 Workpiece: Stainless Steel

Stainless steel is well known because of its corrosion and oxidation resistance due to the chromium-rich oxide layer on the surface layer of alloyed steel. Besides that, it is also tougher and has higher ductility besides having higher hot strength which means, it can operate at high temperatures and retain its strength. Figure 1 shows the stainless-steel workpiece used in the experiment and the EDM machine used for the experiment. Copper was utilized as the electrode material and tool in this study. Copper's high thermal and electrical conductivity make it a desirable material. It is an excellent thermal conductor, electrical conductor, building material, and alloying component.

Figure 2 illustrates the copper workpiece used in the experiment. It has a dimension of 50mm x 30mm x 10mm. As we required a parallel and less distorted contact surface of 10mm x 10mm, the electrode was cut by wire EDM. They were also ground to ensure that the adjacent surfaces are parallel. A total of 6 electrodes are prepared.



Fig. 1. Stainless-steel workpiece

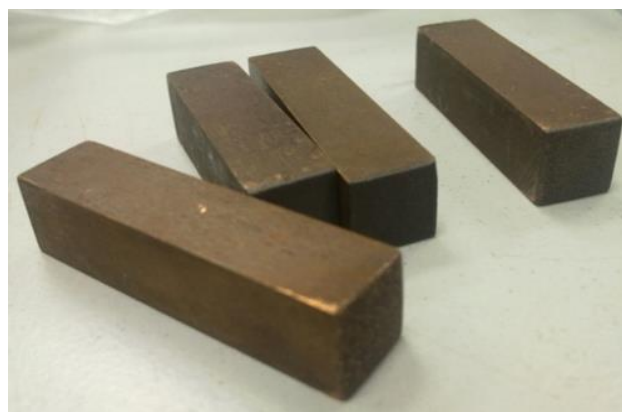


Fig. 2. Copper Electrode

### 2.2 Powder: Tantalum Carbide (TaC)

Extremely hard, with a Mohs scale hardness of 9–10. Only diamond is harder than this material. It is sometimes added to tungsten carbide alloys as a fine-crystalline additive. It's status as the stoichiometric binary compound with the highest measured melting point of 3880 °C. The melting point of the sub-stoichiometric compound TaC is higher, hovering around 4000 degrees Celsius. As a result, it produces a spectacular flash when exposed to air and is only marginally soluble in acids.

### 2.3 Dielectric Fluid

Die-sinking EDM uses kerosene as a dielectric fluid for its tool wear, precision, and surface quality benefits. A dielectric fluid can cool the eroded particles between the workpiece and the electrode and act as a spark dielectric barrier. Kerosene is the dielectric fluid for the experiments because of these qualities.

## 2.4 Design of Experiment (DOE)

The analysis of experimental data, as opposed to theoretical models, is at the heart of experimental design, which is a strategy for acquiring empirical knowledge. It can be used whenever more information is needed about a phenomenon, or when existing information needs to be upgraded. The first steps in designing an experiment are to establish its goal and to decide on the process variables and study outcomes.

This study uses DOE's factorial design and response surface methodology (RSM). RSM models input/output relationships empirically using polynomials as local approximations.

## 2.5 Process Parameters

In any DOE, determining the process parameter is the key. Table 1 discloses the process parameters that have been used for the experimentation. From Table 1, it can be seen that there are four factors which are concentrations, peak current, on-time, and off-time. Table 2 shows the 5 levels of input parameters.

**Table 1**

Parameters and level values were selected for the experiments

Parameter/Factors	Low value	High value
Concentration (TaC), $C_t$	5g/L	45g/L
Peak Current, $I_p$	2A	8A
On-Time, $T_{on}$	5.5 $\mu$ s	7.1 $\mu$ s
Off-Time, $T_{off}$	6.0 $\mu$ s	8.0 $\mu$ s

**Table 2**

Values of machining variable and levels

Variables	Levels				
	-2	-1	0	1	2
Concentration (TaC), $C_t$	5	15	25	35	45
Peak Current, $I_p$	2	3.5	5	6.5	8
On-Time, $T_{on}$	5.5	5.9	6.3	6.7	7.1
Off-Time, $T_{off}$	6	6.5	7	7.5	8

## 2.6 MRR

The volumetric amount of material removed from the workpiece per unit of time is known as the material removal rate (MRR). The standard unit of measurement is cubic millimeters per minute ( $\text{mm}^3/\text{min}$ ). MRR is defined as the weight difference between the workpiece before and following machining divided by the machining time.

## 2.7 Machine Setup

A Mitsubishi EX22 die-sinking EDM machine is used in the experiment. Jet flushing was adequate for our experiment. The setup that was used in all the experiments is shown in Figure 3. The following section comprises the setup procedure (preparation of experimentation) of the EDM machine.



**Fig. 3.** MITSUBISHI EX22 die-sinking EDM

Firstly, the experimental setup is prepared as shown in Figure 3. To limit the excess use of powder and as well as dielectric fluid (kerosene), instead of using the whole tank, a comparatively smaller (250 × 250 × 100 mm) container is used where the machining takes place. To avoid sedimentation of powder particles at the bottom, a stirring system is provided in terms of air flushing. Then, both the workpiece and tool are weighed using a single pan electric balance, and their weights are recorded. A corresponding weight of TaC powder is measured using the same electric balance to get the required concentration. Next, the workpiece is a fixture within the container where a suitable concentration of powder-mixed kerosene dielectric has been added based on the DOE. Meanwhile, the tool is mounted on the tool holder of the Mitsubishi EX22 die-sinking EDM machine. The input parameters are entered and the EDM process started. After each experiment/run the machining time is recorded. After each experiment/run, the workpiece and tool are weighed. The difference in weight is used to calculate MRR and TWR.

### **3. Results and Discussions**

#### **3.1 Analysis of Variance for MRR Models**

Lack-of-fit tests for the proposed model using analysis of variance (ANOVA) are carried out to improve the quadratic model which is selected for the  $MRR_{PMEDM}$ , the insignificant model terms of A, B, C, AB, AC, and  $A^2$  were accepted only from the model. The resulting ANOVA table is shown in Table 3. In the same manner, insignificant model terms in the quadratic model for  $MRR_{EDM}$  (Table 4) were removed. The p-value (Prob>F) column of Table 3 shows p-values of 0.0001 for the model which is less than 0.05. The p-values (Prob>F) of the significant model terms A, B, C, AB, AC, and  $A^2$  are all less than 0.05. In the same way, all significant results must have a value for (Prob>F) that is less than 0.05.  $P > 0.05$  shows how likely it is that the null hypothesis is right. The probability that the other theory is right is equal to 1 minus the P value. If the test result is statistically significant ( $P < 0.05$ ), the test hypothesis is unreliable or should be rejected. If the P value is more than 0.05, it means that there was no effect.

**Table 3**  
 Analysis of variance for  $MRR_{PMEDM}$  (reduced model)

Analysis of variance table [Partial sum of squares - Type III]						
Source	Sum of Squares	df	Mean Square	F Value	p-value Prob > F	
Model	4517.46	7	645.35	208.53	< 0.0001	significant
A-Current	3403.83	1	3403.83	1099.86	< 0.0001	
B-On-Time	304.19	1	304.19	98.29	< 0.0001	
C-Off-Time	420.89	1	420.89	136.00	< 0.0001	
AB	128.12	1	128.12	41.40	< 0.0001	
AC	113.12	1	113.12	36.55	< 0.0001	
A <sup>2</sup>	136.97	1	136.97	44.26	< 0.0001	
C <sup>2</sup>	20.22	1	20.22	6.53	0.0180	
Residual	68.09	22	3.09			
Lack of Fit	55.84	17	3.28	1.34	0.4000	not significant
Pure Error	12.25	5	2.45			
Cor Total	4585.55	29				

**Table 4**  
 Analysis of variance for  $MRR_{EDM}$  (reduced model)

Analysis of variance table [Partial sum of squares - Type III]						
Source	Sum of Squares	df	Mean Square	F Value	p-value Prob > F	
Model	388.57	3	129.52	6.58	0.0042	significant
A-Current	358.98	1	358.98	18.23	0.0006	
B-On-time	5.24	1	5.24	0.27	0.6130	
C-Off-time	24.35	1	24.35	1.24	0.2826	
Residual	315.10	16	19.69			
Lack of Fit	315.10	11	28.65		0.400	not significant
Pure Error	0.000	5	0.000			
Cor Total	703.66	19				

### 3.2 Developed Model for the MRR

The model developed for MRR after the analysis of the response is shown in equations respectively for EDMed with TaC and without TaC powder additive.

The equation developed for  $MRR_{PMEDM}$

$$MRR_{PMEDM} = + 15.59 + 11.91 A + 3.56 B - 4.19 C + 2.83 AB - 2.66 AC + 2.19 A^2 + 0.84 C^2 \quad (1)$$

$$MRR_{PMEDM} = + 192.56337 - 6.70917 \text{ Current} - 14.68096 \text{ On-Time} - 37.86496 \text{ Off-Time} + 4.71626 \text{ Current} * \text{ On-Time} - 3.54523 \text{ Current} * \text{ Off-Time} + 0.97527 \text{ Current}^2 + 3.37255 \text{ Off-Time}^2 \quad (2)$$

The equation developed for  $MRR_{EDM}$

$$1/\text{Sqrt}(MRR)_{EDM} = + 0.27 - 0.088 A - 5.088E-003 B + 0.013 C - 0.042 BC + 0.051 A^2 \quad (3)$$

$$1/\text{Sqrt}(MRR)_{EDM} = - 8.12463 - 0.28717 \text{ Current} + 1.44220 \text{ On-time} + 1.33458 \text{ Off-time} - 0.20785 \text{ On-time} * \text{ Off-time} + 0.022883 * \text{ Current}^2 \quad (4)$$

### 3.3 Adequacy Test for the Developed MRR Model

The model's significance was confirmed by MRR model adequacy checks, which showed that "Lack of fit" is not significant. The model must thus fit the response data, according to this. Table 5 shows adjusted R-squared for the models is more than 0.7. Furthermore, Adj R-squared values of 98.04% and 87.94% observed variability in  $MRR_{PMEDM}$  and  $MRR_{EDM}$  respectively can be explained by the significant model terms of (A, B, C, AB, AC, and  $A^2$ ) and (A, BC, and  $A^2$ ) for the two conditions of MRR. It is advised for models to be sufficient if the difference between the adjusted and predicted R-squared is less than 0.2.

**Table 5**  
 Summary Statistic for MRR

Condition	$MRR_{EDM}$	$MRR_{PMEDM}$
$R^2$	0.9111	0.9852
Adj $R^2$	0.8794	0.9804
Pred $R^2$	0.6993	0.9655
Adeq Precision	20.672	52.437

Further confirming the model's adequacy is that the adequate precision of the two models is more than 4 (Table 5). Model adequacy check for normally distributed residuals is shown on a normal probability plot, where points follow a straight line. Figure 4(a) and Figure 4(b) show this by scattering residuals along a straight line. The residuals are normally distributed.

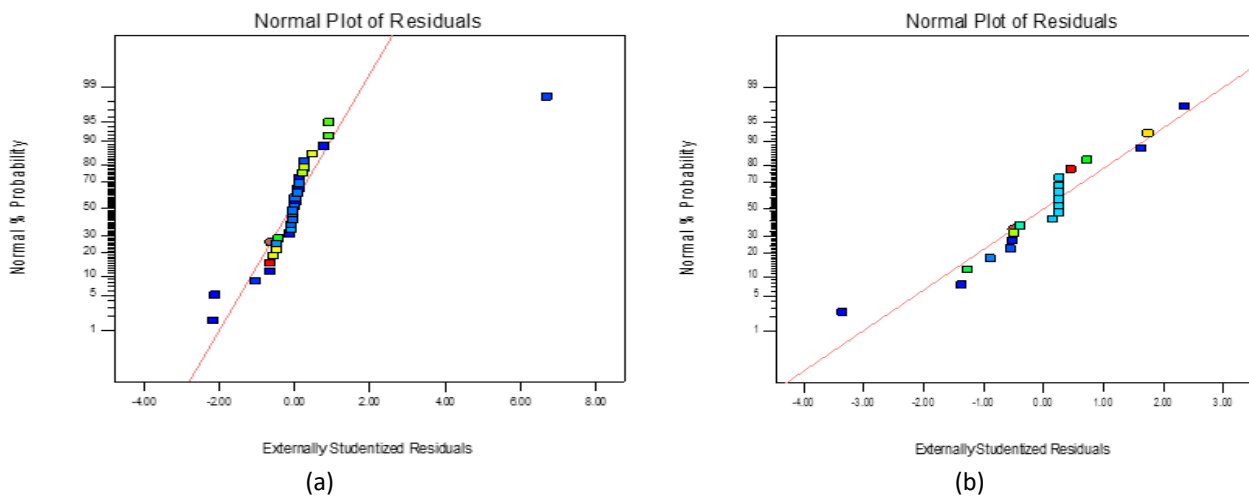


**Fig. 4.** Normal probability of residuals for (a)  $MRR_{PMEDM}$  and (b)  $MRR_{EDM}$

### 3.4 3-Dimensional Surface Plots for $MRR_{PMEDM}$

Figure 5 displays the 3-Dimensional surface and contour plots for the  $MRR_{PMEDM}$ . For the  $MRR_{PMEDM}$  model, it can be seen in Eq. (1) and Eq. (2) that there is an interaction between current and pulse on-time (AB) as well as between current and pulse off-time (AC). Figure 5 also shows that by increased current (A),  $MRR_{PMEDM}$  will increase to a maximum and factor on-time (B) only affect at low values. Figure 5 shows current is the major factor influenced and off-time has less effect on  $MRR_{PMEDM}$ . The surface and contour graphs show best  $MRR_{PMEDM}$   $16\text{mm}^3/\text{min}$  can be achieved at current 5 A and on-time  $6.30\ \mu\text{s}$ , off-time  $7.00\ \mu\text{s}$  with powder concentration  $25\text{g/L}$ .

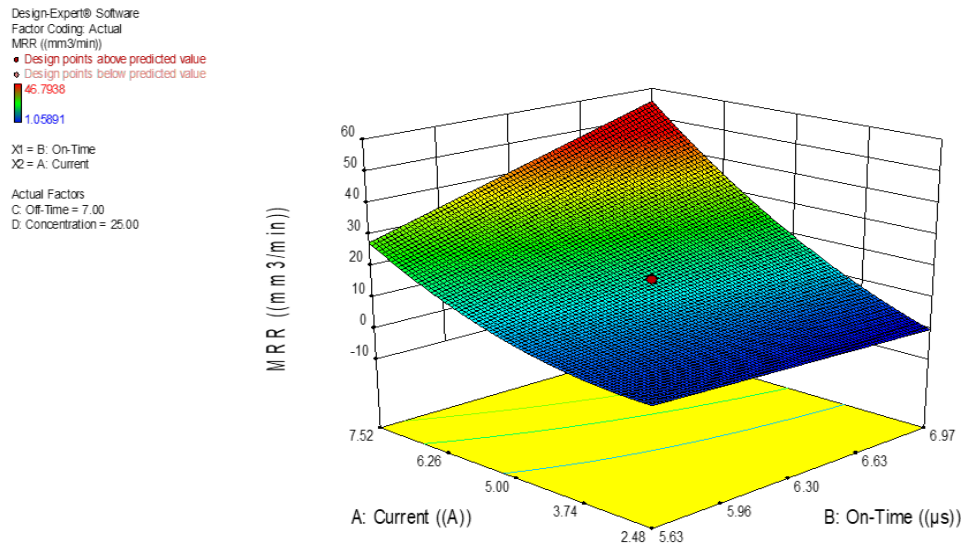


Fig. 5. 3-D surface plots of  $MRR_{PMEDM}$  with current and on time

### 3.5 3-Dimensional Surface plots for $MRR_{EDM}$

The 3-Dimensional surface and contour plots for the  $MRR_{EDM}$  are shown in Figure 6. It can be observed (Eq. (3) and Eq. (4)) for  $MRR_{EDM}$  model that there is an interaction between current and pulse on-time (AB) as well as an interaction between on-time and pulse off-time (AC). Figure 6 also shows that by increased current (A),  $MRR_{EDM}$  will increase in a quadratic pattern where at current 6.26  $\mu$ s,  $MRR_{EDM}$  starts to decrease slightly, and the on-time (B) factor has less effect  $MRR_{EDM}$ .

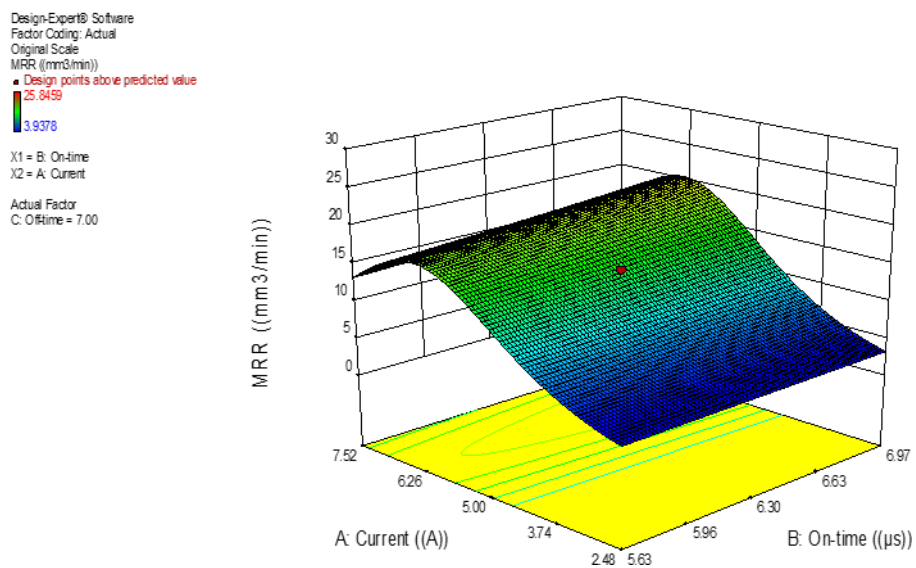
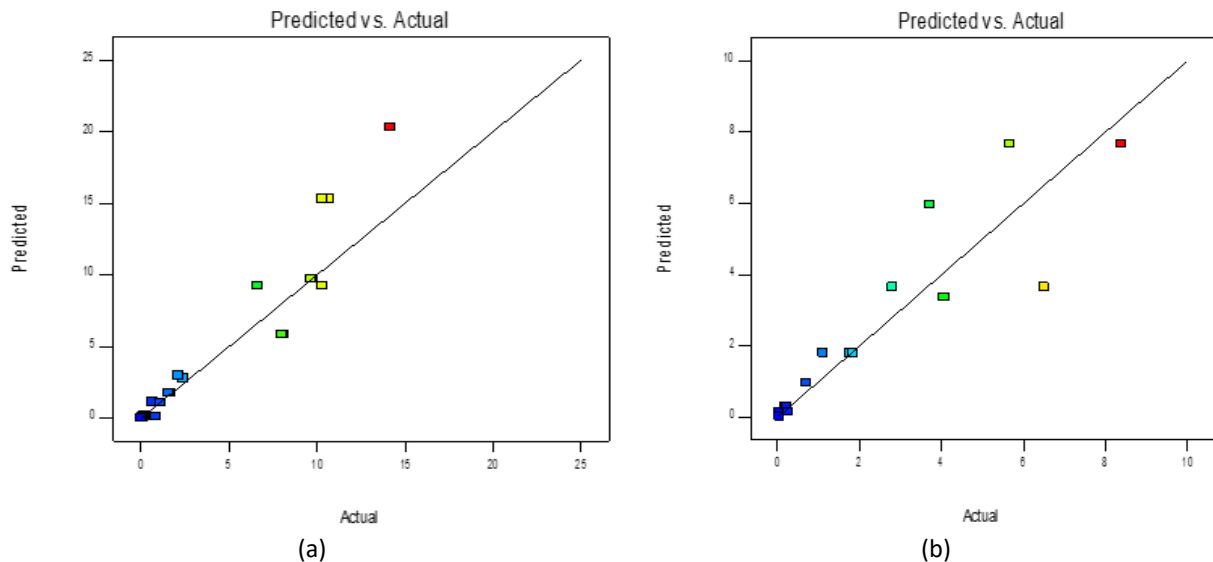


Fig. 6. 3-D surface plots of  $MRR_{EDM}$  with current and on time

### 3.6 Model Predictability for MRR

Figure 7(a) and Figure 7(b) show the plots of predicted against actual response values for MRR. The scattered straight-line nature of the plot confirms the model's adequacy. It shows a close variation between the actual and predicted values of TWR for the two conditions with and without TaC.



**Fig. 7.** Scattered plots of predicted against the measured values for (a)  $MRR_{PMEDM}$  and (b)  $MRR_{EDM}$

### 3.7 Analysis of Variance for TWR Models

Lack-of-fit tests for the proposed model using analysis of variance (ANOVA) are carried out to improve the quadratic model which is selected for the  $TWR_{PMEDM}$ , the insignificant model terms of A, B, C, and  $A^2$  were accepted only from the model. The resulting ANOVA table is shown in Table 6. In the same manner, insignificant model terms in the quadratic model for  $TWR_{EDM}$  (Table 6) were removed. The p-value (Prob>F) column of Table 6 shows p-values of 0.0001 for the model which is less than 0.05. The p-values (Prob>F) for model terms A, B, C, and  $A^2$  that are important are all less than 0.05. In the same way, the model and model terms A, B, and  $A^2$  in Table 6 are all significant when (Prob>F) is less than 0.05. If  $P > 0.05$ , then the null hypothesis is likely to be true. The chance that the other hypothesis is true is equal to 1 minus the P value. If the test result is statistically significant ( $P < 0.05$ ), it means that the test hypothesis is wrong and should be rejected. If the P value is more than 0.05, it means that there was no effect.

**Table 6**  
 Analysis of variance for  $TWR_{PMEDM}$  (reduced model)

Analysis of variance table [Partial sum of squares - Type III]						
Source	Sum of Squares	df	Mean Square	F Value	p-value Prob > F	
Model	117.33	4	29.33	106.46	< 0.0001	significant
A-Current	108.59	1	108.59	394.11	< 0.0001	
B-On-Time	1.22	1	1.22	4.44	0.0452	
C-Off-Time	1.55	1	1.55	5.62	0.0257	
$A^2$	5.97	1	5.97	21.66	< 0.0001	
Residual	6.89	25	0.28			
Lack of Fit	6.88	20	0.34	223.79	0.153	not significant
Pure Error	7.686E-003	5	1.537E-003			
Cor Total	124.22	29				

### 3.8 Developed Model for the TWR

The developed models for TWR with and without TaC after removing the insignificant factors are shown in Eq. (5) and Eq. (6) respectively.

The equation for  $TWR_{PMEDM}$

$$\ln (TWR)_{PMEDM} = + 0.45 + 2.13 A - 0.23 B - 0.25 C - 0.46 A^2 \quad (5)$$

$$\ln (TWR)_{PMEDM} = - 4.58472 + 3.44111 \text{ Current} - 0.56462 \text{ On-Time} - 0.50816 \text{ Off-Time} - 0.20230 \text{ Current}^2 \quad (6)$$

The equation developed for  $TWR_{EDM}$

$$\ln (TWR)_{EDM} = + 0.49 + 1.61 A - 0.3 B - 0.54 A^2 \quad (7)$$

$$\ln (TWR) = - 4.99050 + 3.45160 \text{ Current} - 0.92502 \text{ On-time} - 0.23789 \text{ Current}^2 \quad (8)$$

### 3.9 Adequacy Test for the Developed TWR Model

Lack-of-fit, R-squared, adjusted R-squared, predicted R-squared, and adequate precision statistics are used to check model adequacy. Table 7 shows no "lack of fit." The TWR quadratic models fit response data well. The adjusted R-squared ( $Adj R^2$ ) is greater than 0.7 and the difference between the adjusted and predicted R-squared is less than 0.2. Table 7 shows that significant model terms explain 93.57% of  $TWR_{PMEDM}$ 's observed variability (A, B, C, and  $A^2$ ). For  $TWR_{EDM}$ , A, B, and  $A^2$  explain 91.0% of model variability.

**Table 7**  
 Summary Statistic for TWR

Condition	$TWR_{EDM}$	$TWR_{PMEDM}$
$R^2$	0.9242	0.9445
Adj $R^2$	0.9100	0.9357
Pred $R^2$	0.8353	0.9193
Adeq Precision	27.489	39.704
Lack-of-fit	0	0

Further confirming the model's adequacy is that the adequate precision of the two models is more than 4 (Table 7). Model adequacy check for normally distributed residuals is shown on a normal probability plot, where points follow a straight line. Figure 8(a) and Figure 8(b) show this by scattering residuals along a straight line. The residuals are normally distributed.

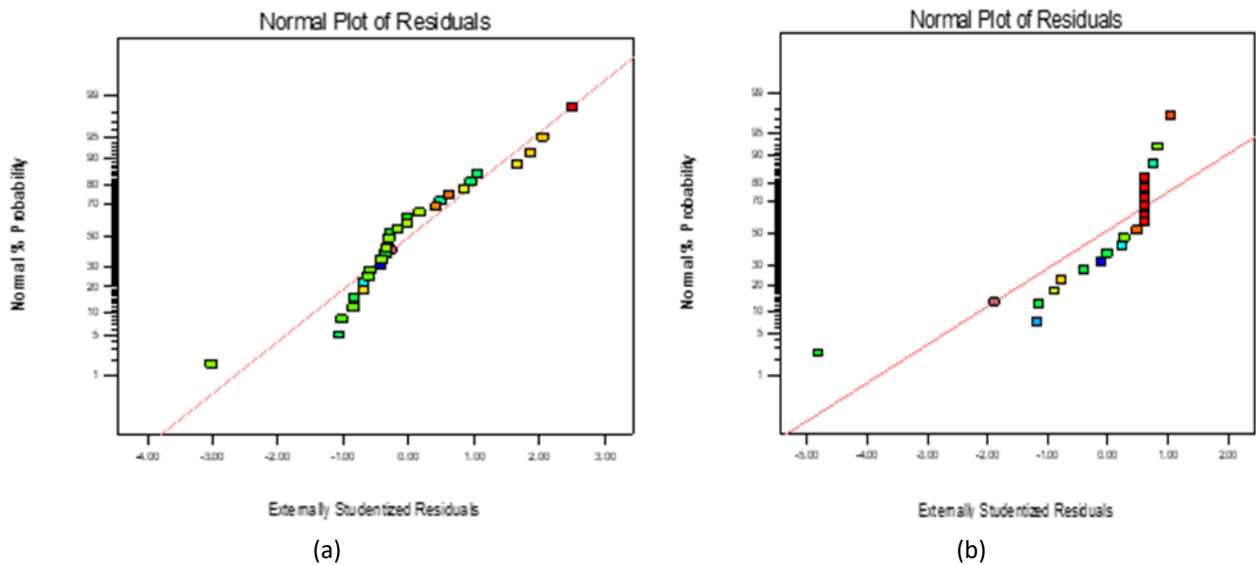


**Fig. 8.** Scattered plots of predicted against the measured values for (a)  $TWR_{PMEDM}$  and (b)  $TWR_{EDM}$

The 3-Dimensional surface plots are used to check the interactions between two factors in the model. It can be seen that for  $TWR_{PMEDM}$  (Eq. (5) and Eq. (6)) significant interactions exist between current and on-time (AB) and off-time (AC). Figure 9(a) shows the 3-Dimensional and the corresponding surface plots for the model developed for  $TWR$ . The curved shapes of the plots are a result of the quadratic effects and the interactions between the factors. Figure 9(a) also shows the surface and contour graphs model suggests the best  $TWR_{EPMEDM}$   $4\text{mm}^3/\text{min}$  achieved at current 5 A, on-time  $6.30\ \mu\text{s}$  and off-time  $7.00\ \mu\text{s}$  with powder TaC powder concentration  $25\text{g/L}$ . This means that the effect of on-time and off-time is equal versus current in  $TWR_{PMEDM}$ , because of existing of TaC powder in the dielectric medium.

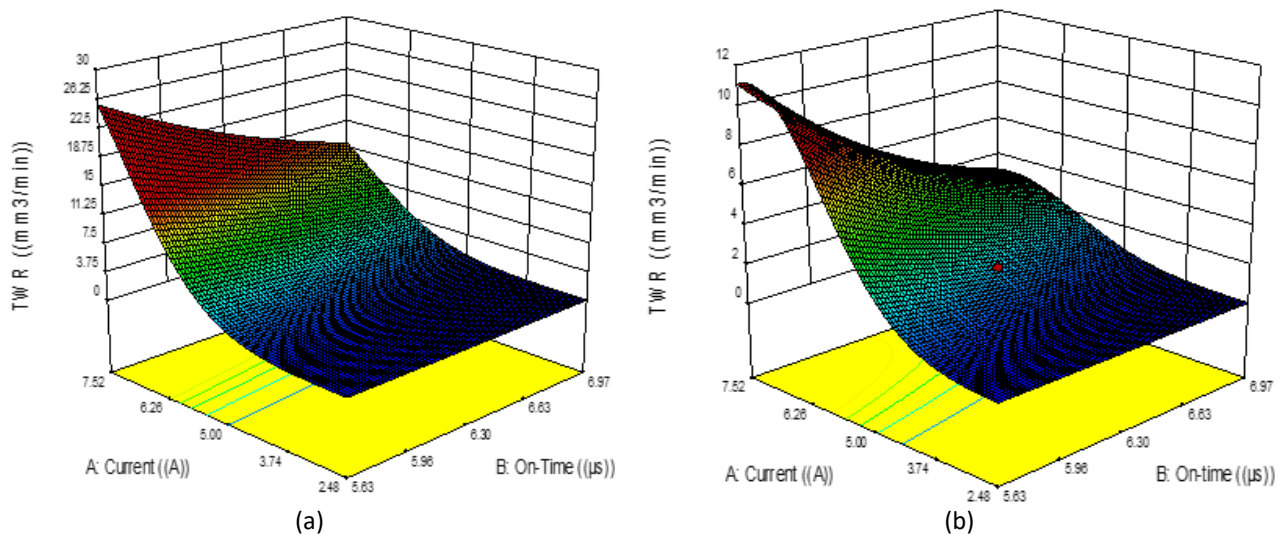


**Fig. 9.** 3-D surface plots of a)  $TWR_{PMEDM}$  with current and on time b)  $TWR_{EDM}$  with current and on time

The significant interaction of the 3-Dimensional surface plot for the model developed for  $TWR_{EDM}$  (Eq. (7) and Eq. (8)) is shown in Figure 9(b). As explained for the  $TWR_{PMEDM}$  model, Figure 9(b) shows that there is an interaction between current and pulse on-time (AB) for  $TWR_{EDM}$  model. This shows that the effect of pulse on time on  $TWR_{EDM}$  depends on the level of current. The corresponding contour plot for the 3-Dimensional surface shows that the interaction and the quadratic terms in the

model produced the curve shape in Figure 9(b). It also shows contour graphs model suggests the best  $TWR_{EDM}$   $1.8\text{mm}^3/\text{min}$  achieved at current 5 A, on-time  $6.30\ \mu\text{s}$  and off-time  $7.00\ \mu\text{s}$ .

### 3.10 Optimization of MRR and TWR

In the case of PMEDM optimization, Table 8 shows that the optimum pulse on-time and pulse off-time are  $6.20\ \mu\text{s}$  and  $6.50\ \mu\text{s}$  respectively. The results also conclude that the optimum value for concentration is  $35\text{g/L}$ . From the results in Table 8, it may also be concluded that minimum TWR and maximum MRR can be achieved at  $81.98\%$  and  $13.779\text{mm}^3/\text{min}$  respectively with  $83.50\%$  desirability.

**Table 8**

Optimization solutions generated for  $TWR_{PMEDM}$ , and  $MRR_{PMEDM}$

Number	Current	On-Time	Off-Time	Concentration	TWR	MRR	Desirability	
1	4.303	6.203	6.500	35.000	0.819	13.779	0.835	Selected
2	4.303	6.195	6.500	35.000	0.822	13.730	0.835	
3	4.298	6.189	6.500	35.000	0.818	13.658	0.835	
4	4.303	6.219	6.500	35.000	0.812	13.868	0.835	
5	4.310	6.183	6.500	35.000	0.838	13.724	0.835	

While EDM machining the stainless steel workpiece without TaC powder additive, the optimization results in Table 9 show that the optimum current is also 4.64 A, while the pulse on-time is set at  $5.90\ \mu\text{s}$  and pulse off-time  $6.50\ \mu\text{s}$ . Moreover, Table 9 shows solution No.1 that the optimum response variables resulting from the optimized machining parameters are TWR gives  $1.733\%$  and MRR is  $17.11\ \text{mm}^3/\text{min}$ .

**Table 9**

Optimization solutions generated for  $TWR_{EDM}$  and  $MRR_{EDM}$

Number	Current	On-time	Off-time	MRR	TWR	Desirability	
1	4.643	5.900	6.500	17.111	1.733	0.579	Selected
2	4.630	5.900	6.500	16.971	1.705	0.579	
3	4.653	5.900	6.500	17.225	1.756	0.579	
4	4.666	5.900	6.500	17.365	1.783	0.579	
5	4.690	5.900	6.500	17.631	1.837	0.578	

## 4. Conclusions

The following are some inferences that can be made in light of the findings and the discussion is that according to the MRR model for EDM with TaC powder additive, the current has the greatest impact, followed by pulse on-time and pulse off-time. Although insignificant, concentration is found to have some indirect effects. The current, followed by pulse off-time and pulse on-time, has the greatest impact on MRR in the case of MRR without TaC powder additive ( $MRR_{EDM}$ ). The model predicts that concentration is a minor factor in  $MRR_{EDM}$  conditions. When machining stainless steel with an electrical discharge, TaC powder additive is a viable alternative for boosting MRR and lowering tool wear (SUS 304). The  $MRR_{PMEDM}$  increase ranges from 4.3 to 5.3%, and  $TWR_{PMEDM}$  was reduced by 37.9%. Optimized results also show that TWR and maximum MRR can be achieved at  $81.98\%$  and  $13.779\text{mm}^3/\text{min}$  respectively with  $83.50\%$  desirability whenever the pulse on-time and pulse off-time are  $6.20\ \mu\text{s}$  and  $6.50\ \mu\text{s}$  respectively. The models are reliable and can be used to forecast the machining responses within the experimental region, it can be said. TaC powder additive

improves EDM technological responses, including the effective rate of material removal, when used with stainless steel.

### Acknowledgment

The International Islamic University Malaysia's machining lab, workshop, and metrology lab were used for the research. The author is appreciative of the contemporary lab setting as well as the lab assistant's assistance.

### References

- [1] Abu Qudeiri, Jaber E., Abdel-Hamed I. Mourad, Aiman Ziout, Mustufa Haider Abidi, and Ahmed Elkaseer. "Electric discharge machining of titanium and its alloys." *The International Journal of Advanced Manufacturing Technology* 96 (2018): 1319-1339. <https://doi.org/10.1007/s00170-018-1574-0>
- [2] Talla, Gangadharudu, S. Gangopadhyay, and C. K. Biswas. "State of the art in powder-mixed electric discharge machining: a review." *Proceedings of the Institution of Mechanical Engineers, Part B: Journal of Engineering Manufacture* 231, no. 14 (2017): 2511-2526. <https://doi.org/10.1177/0954405416634265>
- [3] Al-Amin, Md, Ahmad Majdi Abdul Rani, Abdul Azeez Abdu Aliyu, Muhammad Al'Hapis Abdul Razak, Sri Hastuty, and Michael G. Bryant. "Powder mixed-EDM for potential biomedical applications: A critical review." *Materials and Manufacturing Processes* 35, no. 16 (2020): 1789-1811. <https://doi.org/10.1080/10426914.2020.1779939>
- [4] Mahmud, Nazriah, and Azli Yahya. "Consistent Machining of Electrical Discharge Machining Power Supply Towards Hip Implant Surface Texturing." *Journal of Advanced Research in Applied Sciences and Engineering Technology* 11, no. 1 (2018): 39-46.
- [5] Ali, M. A. Md, S. Laily, B. Manshoor, N. I. Syahrian, R. Izamshah, M. Hadzley, and M. R. Muhamad. "Performance of copper, copper tungsten, graphite and brass electrode on MRR, EWR and SR of aluminium LM6 in EDM die sinking." *Journal of Advanced Research in Applied Mechanics* 6, no. 1 (2015): 30-36.
- [6] Marashi, Houriyeh, Davoud M. Jafarlou, Ahmed AD Sarhan, and Mohd Hamdi. "State of the art in powder mixed dielectric for EDM applications." *Precision Engineering* 46 (2016): 11-33. <https://doi.org/10.1016/j.precisioneng.2016.05.010>
- [7] Rashid, Mir Akmam Noor, Tanveer Saleh, Wazed Ibne Noor, and Mohamed Sultan Mohamed Ali. "Effect of laser parameters on sequential laser beam micromachining and micro electro-discharge machining." *The International Journal of Advanced Manufacturing Technology* 114 (2021): 709-723. <https://doi.org/10.1007/s00170-021-06908-8>
- [8] Noor, Wazed Ibne, Tanveer Saleh, Mir Akmam Noor Rashid, Azhar Mohd Ibrahim, and Mohamed Sultan Mohamed Ali. "Dual-stage artificial neural network (ANN) model for sequential LBMM- $\mu$ EDM-based micro-drilling." *The International Journal of Advanced Manufacturing Technology* 117, no. 11-12 (2021): 3343-3365. <https://doi.org/10.1007/s00170-021-07910-w>
- [9] Joshy, Jino, M. Venkata Krishna Reddy, Basil Kuriachen, and M. L. Joy. "Effect of Powder-Mixed Electric Discharge Alloying Using WS<sub>2</sub> on the Tribological Performance of Ti6Al4V." *Transactions of the Indian Institute of Metals* (2022): 1-12. <https://doi.org/10.1007/s12666-022-02817-w>
- [10] Sudheer, Renumala, M. Venkata Krishna Reddy, Jino Joshy, Basil Kuriachen, and M. L. Joy. "Effect of MoS<sub>2</sub> Powder-Mixed Electric Discharge Alloying on the Tribological Performance of Ti6Al4V." *Transactions of the Indian Institute of Metals* (2022): 1-13. <https://doi.org/10.1007/s12666-022-02786-0>
- [11] Philip, Jibin T., Jose Mathew, and Basil Kuriachen. "Transition from EDM to PMEDM-impact of suspended particulates in the dielectric on Ti6Al4V and other distinct material surfaces: a review." *Journal of Manufacturing Processes* 64 (2021): 1105-1142. <https://doi.org/10.1016/j.jmapro.2021.01.056>
- [12] Khan, Ahsan Ali, Mohammed Baba Ndaliman, Zakaria Mohd Zain, Mohammad F. Jamaludin, and Umar Patthi. "Surface modification using electric discharge machining (EDM) with powder addition." In *Applied Mechanics and Materials*, vol. 110, pp. 725-733. Trans Tech Publications Ltd, 2012. <https://doi.org/10.4028/www.scientific.net/AMM.110-116.725>
- [13] Kung, Kuang-Yuan, Jenn-Tsong Horng, and Ko-Ta Chiang. "Material removal rate and electrode wear ratio study on the powder mixed electrical discharge machining of cobalt-bonded tungsten carbide." *The International Journal of Advanced Manufacturing Technology* 40, no. 1-2 (2009): 95-104. <https://doi.org/10.1007/s00170-007-1307-2>
- [14] Singh, Paramjit, Anil Kumar, Naveen Beri, and Vijay Kumar. "Some experimental investigation on aluminum powder mixed EDM on machining performance of hastelloy steel." *International Journal of Advanced Engineering Technology* 1, no. 2 (2010): 28-45.

- [15] Sharma, Saurabh, Anil Kumar, Naveen Beri, and Dinesh Kumar. "Effect of aluminum powder addition in dielectric during EDM of hastelloy on machining performance using reverse polarity." *International Journal of Advanced Engineering Technology* 1, no. 3 (2010): 13-24.
- [16] Sharma, Saurabh, Anil Kumar, and Naveen Beri. "Study of tool wear rate during powder mixed electrical discharge machining of hastelloy steel." *International Journal of Advanced Engineering Technology* 2, no. 2 (2011): 133-139.
- [17] Chatha, Sukhpal S., Rakesh Bhatia, and Hazoor S. Sidhu. "Impact of added titanium oxide in dielectric of EDM on surface characteristics and MRR." In *Proc. Nat. Conf. Advancements and Futuristics Trends in Mech. Mater. Eng.* 2010.
- [18] Pecas, Paulo, and Elsa Henriques. "Influence of silicon powder-mixed dielectric on conventional electrical discharge machining." *International Journal of Machine Tools and Manufacture* 43, no. 14 (2003): 1465-1471. [https://doi.org/10.1016/S0890-6955\(03\)00169-X](https://doi.org/10.1016/S0890-6955(03)00169-X)
- [19] Kansal, H. K., Sehijpal Singh, and Pradeep Kumar. "Performance parameters optimization (multi-characteristics) of powder mixed electric discharge machining (PMEDM) through Taguchi's method and utility concept." *Indian Journal of Engineering and Materials Sciences* 13 (2006): 209-216.
- [20] Furutania, Katsushi, Akinori Saneto, Hideki Takezawa, Naotake Mohri, and Hidetaka Miyake. "Accretion of titanium carbide by electrical discharge machining with powder suspended in working fluid." *Precision Engineering* 25, no. 2 (2001): 138-144. [https://doi.org/10.1016/S0141-6359\(00\)00068-4](https://doi.org/10.1016/S0141-6359(00)00068-4)